ELSEVIER

Earth and Planetary Science Letters 190 (2001) 93–101

EPSL

www.elsevier.com/locate/epsl

The effect of temperature, pressure, and sulfur content on viscosity of the Fe–FeS melt

Hidenori Terasaki [a,*], Takumi Kato [a], Satoru Urakawa [b], Ken-ichi Funakoshi [c], Akio Suzuki [d], Taku Okada [e], Makoto Maeda [d], Jin Sato [d], Tomoaki Kubo [d], Shidu Kasai [d]

[a] *Geoscience Institute, University of Tsukuba, Tsukuba 305-8571, Japan*
[b] *Department of Earth Sciences, Okayama University, Okayama 700-8530, Japan*
[c] *Japan Synchrotron Radiation Research Institute, Hyogo 679-5198, Japan*
[d] *Institute of Mineralogy Petrology and Economic Geology, Tohoku University, Sendai 980-8578, Japan*
[e] *Japan Atomic Energy Research Institute, Hyogo 679-5148, Japan*

Received 28 November 2000; received in revised form 2 May 2001; accepted 9 May 2001

Abstract

The Fe–FeS melt is thought to be the major candidate of the outer core material. Its viscosity is one of the most important physical properties to study the dynamics of the convection in the outer core. We performed the in situ viscosity measurement of the Fe–FeS melt under high pressure using X-ray radiography falling sphere method with a novel sample assembly. Viscosity was measured in the temperature, pressure, and compositional conditions of 1233–1923 K, 1.5–6.9 GPa, and Fe–$Fe_{72}S_{28}$ (wt%), respectively. The viscosity coefficients obtained by 17 measurements change systematically in the range of 0.008–0.036 Pa s. An activation energy of the viscous flow, $Q = 30.0 \pm 8.6$ kJ/mol, and the activation volume, $\Delta V = 1.5 \pm 0.7 \times 10^{-6}$ m^3/mol, are determined as the temperature and pressure dependence, and the viscosity of the $Fe_{72}S_{28}$ melt is found to be smaller than that of the Fe melt by $15 \pm 10\%$. These tendencies can be well correlated with the structural variation of the Fe–FeS melt.

Keywords: viscosity; iron-sulfides; melts; autoradiography; high pressure; outer core

1. Introduction

The Earth's outer core consists mainly of liquid Fe–Ni alloy with a significant amount of the light elements such as S, O, C, Si, and H [1–3]. Among them, sulfur is considered to be the major candidate of the light element in the outer core [3]. Therefore, it is important to study the effect of temperature, pressure, and sulfur content on the viscosity coefficient of the Fe–FeS melt in the wide ranges of conditions.

LeBlanc and Secco [4] measured the viscosity of the Fe–FeS eutectic melt ($Fe_{73}S_{27}$) using the electro-detection falling sphere method at 2–5 GPa and 1373–1573 K. According to their results, viscosity coefficients are 0.5–14 Pa s and the values are higher by 2–3 orders of magnitude than those

* Corresponding author. Tel.: +81-298-53-7352; Fax: +81-298-53-7352; E-mail: terasaki@davidbowie.com

0012-821X/01/$ – see front matter
PII: S0012-821X(01)00374-0

of Fe and FeS melts at ambient pressure (Lucas [5] and Barmin et al. [6]).

X-ray radiography falling sphere method (Kanzaki et al. [7]) enables us to directly observe the falling behavior of the marker sphere in the high pressure cell through synchrotron X-ray shadow imaging. Especially for the low viscosity melt, this method is superior to the quenching method (Dingwell [8]). We have applied it to the Fe–FeS eutectic melt ($Fe_{72}S_{28}$) and obtained the viscosity at 6.9 GPa and 1333 K, which was comparable to the atmospheric pressure values (Urakawa et al. [9]). Recent measurement with the similar method by Dobson et al. [10] on the FeS and Fe–FeS eutectic melt up to 5 GPa also indicated similar results.

Continuous effort has been made to improve the accuracy of the viscosity measurement and to clarify quantitatively the effect of temperature, pressure, and sulfur content on the viscosity. In this study, in situ viscosity measurements have been conducted in the ranges of 1.5–6.9 GPa, 1233–1923 K, and Fe–$Fe_{72}S_{28}$ composition. Technical improvement using a new sample assembly realized viscosity measurement at high temperatures and increased reliability of the measured values. The results were used to obtain the thermodynamic parameters of the temperature and pressure dependence and the compositional dependence in the range between pure Fe and eutectic. Their correlation with the structural variation of the melt and comparisons with the previous study are also discussed.

2. Experimental procedure

High pressure and temperature experiments were performed by MA-8 multianvil press system (SPEED-1500) installed at BL04B1, SPring-8, Japan [11]. 8 mm truncated-edge-length tungsten carbide anvils were used with a Cr_2O_3 doped MgO semi-sintered octahedron pressure medium, 14 mm in size. Starting material was a mixture of Fe (Rare Metallic Co., Ltd., 4N) and FeS (Rare Metallic Co., Ltd., 3N) powders, and its composition was $Fe_{72}S_{28}$ (weight ratio), which corresponds to the eutectic composition at atmospheric

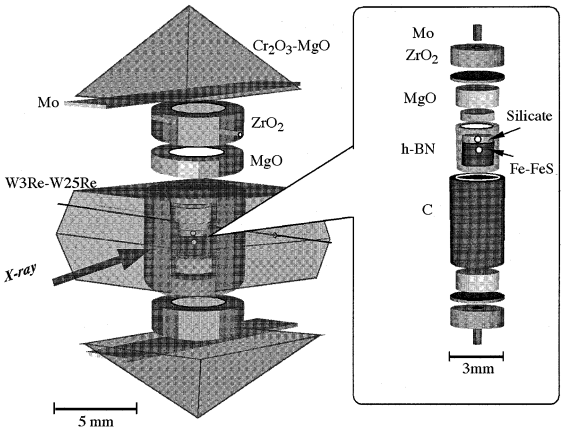

Fig. 1. Schematic diagrams of the 2 step falling sphere cell assembly.

pressure. We also used $Fe_{80}S_{20}$, $Fe_{87}S_{13}$, and Fe_{100} compositions to investigate the effect of S content on the viscosity. Fig. 1 shows the schematic image of the cell assembly. Experimental pressure was determined from the equation of state for hexagonal-boron nitride (Urakawa et al. [12]), which was used as a sample capsule. The h-BN is one of the proper internal pressure standards at temperatures higher than 1273 K and pressures lower than 10 GPa, because it has a high melting point and a slow grain growth rate at high temperature. Further, it is chemically inert with both of Fe–FeS and silicate samples. The h-BN capsule was deoxidized in advance with the induction heater at 2273 K with N_2 flow. The heater was made of cylindrical graphite. X-ray window and thermal insulator around the heater was composed of MgO and ZrO_2, respectively. Molybdenum foil and rod were used as a electrode. Temperature was monitored by the W3%Re–W25%Re thermocouple, of which junction was positioned just above the h-BN capsule inside the heater. No correction was made for the effect of pressure on the electromotive force.

Viscosity was measured by the X-ray radiography falling sphere method (Kanzaki et al. [7]). Using white X-ray, transmitted beam was transferred to visible light by the YAG fluorescent disc and then detected by the high-speed exposure CCD camera (C4880-80-14A, Hamamatsu Photonics K.K.). Images of the falling sphere were

observed with a resolution of about 5 μm and with the exposure time of 29 ms, and were recorded by the computer with the frame grabber board and the video cassette recorder (VCR). Calibration of the distance in the radiographic image was carried out by the records of the stepwise shifts of the press system, which is controlled with a μm step. We used Pt, W, and Au spheres with a diameter of 100–150 μm, as viscosity markers.

After applying pressure, X-ray diffraction of the h-BN was collected for the pressure determination at room temperature. Temperature was raised with the rate of about 100 K/min until 1123 K, which was well below the Fe–FeS eutectic melting point, and then raised to the target value within 1.5 min.

In the usual sample assembly, viscosity measurement is possible only at temperature just above the solidus, especially for the melt with low viscosity. We designed the double-layered assembly (Fig. 1), which consisted of the Fe–FeS and silicate layers in a cell. The silicate layer is positioned at the top of the Fe–FeS sample (Fig. 2). Two spheres were set in a single run as the viscosity markers. One is in the Fe–FeS layer and another is in the silicate layer. During heating, the Fe–FeS starts to melt first, and melting of the silicate at higher temperatures followed. Therefore, the sphere in the silicate layer is held to higher temperature. The run temperatures (T_{1st} and T_{2nd}) correspond to the melting temperatures of the Fe–FeS and the silicate, at which respective spheres start to fall in the Fe–FeS melt. This new technique enables us to study the temperature dependence of the viscosity by changing the silicate composition. We adopted either of albite ($NaAlSi_3O_8$) or, jadeite ($NaAlSi_2O_6$) or, diopside ($CaMgSi_2O_6$) as a material of the silicate layer.

After the falling of the spheres, temperature was kept constant, and the diffraction of h-BN was collected again at the run temperature to determine the run pressure. In some runs, heating was terminated at the initial stage of the falling sphere, or just after the settlement of the sphere. The recovered samples were mounted in epoxy and polished for the scanning electron microscopic observation (JEOL, JSM-5400) and the microprobe analysis (JEOL JXA-8621 electron microprobe).

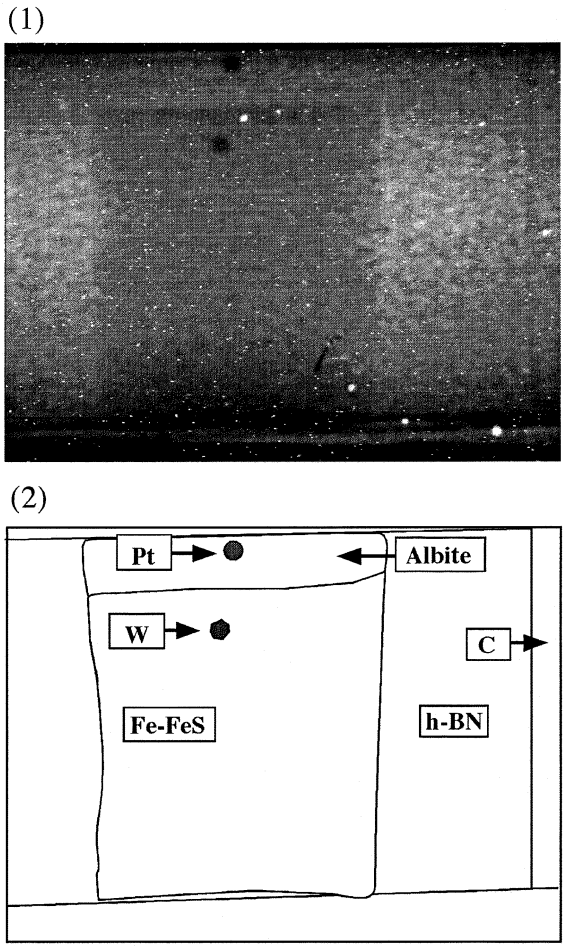

Fig. 2. (1) X-ray radiographic image of 2 step falling sphere cell, showing the clear boundary between sample and silicate. (2) Schematic diagram of (1). The diameter of metal sphere is about 120 μm.

3. Results

Experimental conditions and results are summarized in Table 1. Fig. 3 shows time falling distance profiles for the two spheres. The settling behavior of the lower sphere in the Fe–FeS was divided into two stages (Fig. 3-(1)). In a first stage, the falling velocity is slow with horizontal oscillations and movements, and in a second

stage, it is rapid with a straight vertical path. Microscopic observation of the recovered sample, which was quenched in the initial stage of the falling sphere, showed that the collision with the residual FeS grain caused the irregular movement of the sphere. Thus, the first stage was judged to be in the partial molten state. We adopted the velocity in a second stage as those in the complete molten state. On the other hand, in the falling profile of the second sphere, only a rapid vertical path has been observed (Fig. 3-(2)). It means that the Fe–FeS has completely melted before the second sphere starts to fall.

Textural observation of the above-described sample also provides us a useful constraint on the temperature distribution in the cell. The residual FeS grains concentrate at the vertical center and small areas of complete melting zones are observed at both upper and bottom of the sample. From this textual distribution, the central part is inferred to be a lower temperature, due to thermally conductive MgO window around the heater. The actual maximum temperature difference between the cold center and the hot ends is about 30 K, because the thermocouple reading temperature at the onset of melting in the radiographic image accords with the published phase diagram of the Fe–FeS system. Under such conditions, convection of the molten sample is not likely to occur, as already estimated in the fluid dynamic basis in our previous study [9].

Settling velocity was obtained from the continuous radiographic images, and the viscosity coefficients (η) were calculated using Stokes' equation including the Faxen correction for the effects of the wall (W) and the container end (E) [13,14]:

$$\eta = \frac{2gr_s^2\,(\rho_s-\rho_m)W}{9vE} \quad (1)$$

$$W = 1-2.104\left(\frac{r_s}{r_c}\right)+2.09\left(\frac{r_s}{r_c}\right)^3-0.95\left(\frac{r_s}{r_c}\right)^5 \quad (2)$$

$$E = 1+3.3\left(\frac{r_s}{h_c}\right) \quad (3)$$

where v is the falling velocity, ρ_s and ρ_m are the densities of sphere and sample melt, r_s, r_c are the radius of sphere and capsule, respectively, and h_c is capsule height, taken to be the falling distance. The correction factor of the wall effect (W) is about 0.7–0.9 and that of the end effect (E) is typically about 1.2–1.7, depending on the falling distance.

Sphere size was calculated from the measure-

Table 1
Experimental conditions and results

Run#	P (GPa)	T_{1st} (K)	T_{2nd} (K)	S (wt%)	Silicate layer[a]	v_{1st} (mm/s)	v_{2nd} (mm/s)	η_{1st} (Pa s$\times10^{-2}$)	η_{2nd} (Pa s$\times10^{-2}$)
S350[b,c]	1.5	1253	1623	27.7	Di	2.31	–	1.47(0.59)	–
S308[c]	2.5	1273	1673	27.7	Ab	3.29	7.38	2.66(1.07)	0.91(0.23)
S275	3.5	1303	–	27.7	–	3.19	–	3.56 (1.42)	–
S315	2.7	1258	1503	27.7	Jd	1.91	12.90	2.12(0.85)	0.94(0.24)
S361	3.2	1259	–	27.7	Jd	1.45	–	2.51(1.00)	–
S318[b]	4.7	1353	1813	27.7	Ab	3.39	13.96	2.44(0.98)	0.82(0.21)
S317[c]	4.7	1364	–	27.7	Jd	1.33	–	2.41(0.96)	–
S226[d]	5.0	1373	–	27.7	–	2.69	–	1.60(0.64)	–
S346	5.6	1365	1821	27.7	Ab	2.68	9.32	2.46(0.98)	1.23(0.31)
S230[d]	6.9	1333	–	27.7	–	1.95	–	2.40(0.96)	–
S321	2.7	1323	1669	19.8	Ab		10.15		1.24(0.31)
S325[c]	2.7	1553	1611	12.6	Ab		7.98		1.31(0.33)
S356	2.8	1891	1923	0	Di		6.37		1.76(0.44)

[a]Abbreviation: Ab, albite ($NaAlSi_3O_8$); Jd, jadeite ($NaAlSi_2O_6$); Di, diopside ($CaMgSi_2O_6$).
[b]Temperature was estimated by power–temperature relation.
[c]Pressure of this run was estimated by load–pressure relation referred to the previous experiments.
[d]The same data with those of Urakawa et al. [9].

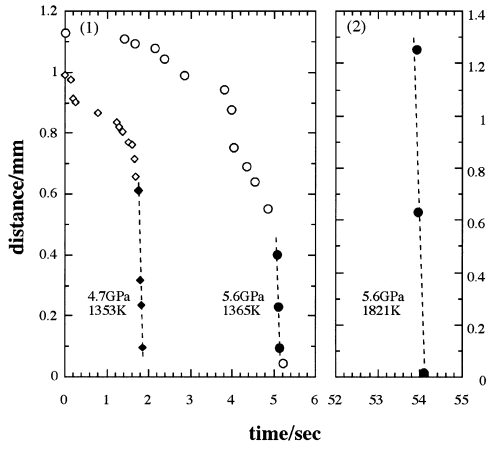

Fig. 3. Falling profiles of run S318 and S346. The width of the anvil gap corresponds to the full scale of the distance. (1) Falling path of the first sphere in the lower layer at 1353 K (diamond) and 1365 K (circle). The data in stage 1 are partial melting indicated by open symbols. Valuable data for viscosity analysis are acquired from the complete melting zone in stage 2 (shown by the closed symbols and the dashed lines). (2) Falling path of the second sphere at 1821 K. Complete melting in the entire path is realized before the falling sphere. The sphere position at the time before the profile is out of frame.

ment by the scanning electron microscopic observation prior to the sampling. Sphere densities of the platinum, tungsten, and gold at high pressure and high temperature were calculated from shock wave data of Jamieson et al. [15], and Walsh [16] using the Mie–Grüneisen equation of state. A density of the Fe–FeS melt was calculated from the density at ambient pressure reported by Nagamori [17] and Hixon et al. [18], and the static compression data of Sanloup et al. [19] using the Birch–Murnaghan equation of state. Capsule size was determined by the radiographic image observation.

We could not find any prominent reaction among the Fe–FeS sample, the capsule (BN) and the silicate materials. A small amount of oxygen ($\sim$0.7 wt%) was detected in the recovered samples. This oxygen may be derived from the oxidized crust of the starting iron powder or the confined air. The dissolved sphere component in the sample melt contributed little to the viscosity because of its negligible amount ($\sim$0.23 wt%).

On the time scale of the chemical reaction between the sample melt and the marker sphere, we have two sources of information: (1) The marker sphere is observed to dissolve into the Fe–FeS melt over a 20–30 s in the in situ radiographic images. (2) In the run products quenched just after the settlement of the falling sphere (2–3 s later), we observed diffusion profiles of the marker sphere component in the Fe–FeS samples, which extended to $\sim$140 μm.

The first marker sphere was in contact with the sample melt for several seconds, so that size reduction up to 10% would be possible. However, the second sphere came from the silicate layer and went through the sample melt within 0.15 s. Accordingly, effect of the chemical reaction would be negligible for the second sphere during the viscosity measurement. We estimated the error arising from the velocity measurement and the calculation of the sample and sphere densities, to be 25%. The effects of the size reduction due to chemical reaction increase the error to 40% for the measurement using the first sphere.

The viscosity coefficients obtained by this study ranged from 8.0×10^{-3} Pa s up to 3.6×10^{-2} Pa s. The present results could successfully be expressed as a function of pressure, temperature, and sulfur content through the following thermodynamic parameterization.

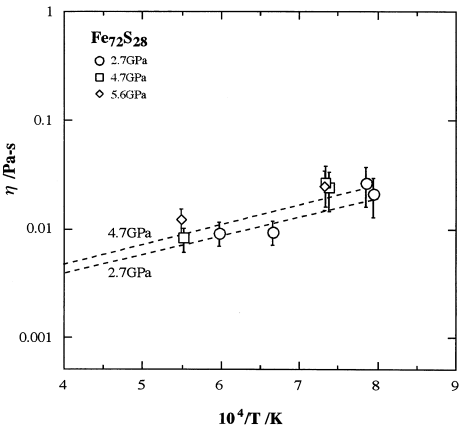

Fig. 4. Temperature dependence of the viscosity coefficient. Each symbols show the viscosity of the $Fe_{72}S_{28}$ melt at different pressures. Dashed lines show the results of the least square fitting of the Arrhenius equation at 2.7 and 4.7 GPa.

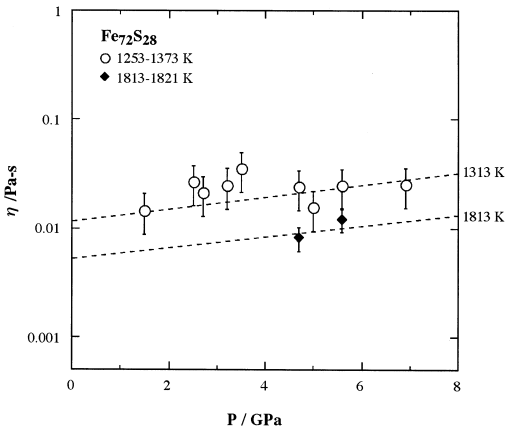

Fig. 5. Pressure dependence of the viscosity coefficient. Open circles, and solid diamonds show the viscosity of the $Fe_{72}S_{28}$ melt at 1253–1373 and 1813–1821 K, respectively. Dashed lines represent the results of the least square fitting of the Arrhenius equation at the corresponding temperatures.

The viscosity data set of the $Fe_{72}S_{28}$ melt was fitted to the following Arrhenius equation:

$$\eta = \eta_0 \exp\left[\frac{Q + P\Delta V}{RT}\right] \quad (4)$$

where R is a gas constant. Activation energy (Q) of viscous flow, activation volume (ΔV), and the pre-potential viscosity factor (η_0) obtained from the least square analysis of the present results are 30.0 ± 8.6 kJ/mol, (1.5 ± 0.7) × 10^{-6} m^3/mol, and (7.5 ± 5.2) × 10^{-4}, respectively.

The effect of temperature on viscosity coefficient of the $Fe_{72}S_{28}$ melt is shown in Fig. 4. It is found that viscosity values of this study decrease with increasing temperature and its dependence is relatively small. Pressure effect on viscosity value is shown in Fig. 5, which indicates a slight increase of the viscosity coefficient with pressure.

Fig. 6 shows the effect of the sulfur content on the viscosity coefficient at 2.7 GPa. We assumed linear dependence of logarithmic scaled viscosity on the sulfur content in the range of 0–28 wt%. The data shows that the viscosity coefficient decreases with the increasing sulfur content and the following equation comprises, $\log \eta = \log \eta^* - CX_s$, where η^* is the Fe viscosity at 2.7 GPa and 1923 K, X_s is the weight fraction of sulfur, and C is constant (0.03 ± 0.008).

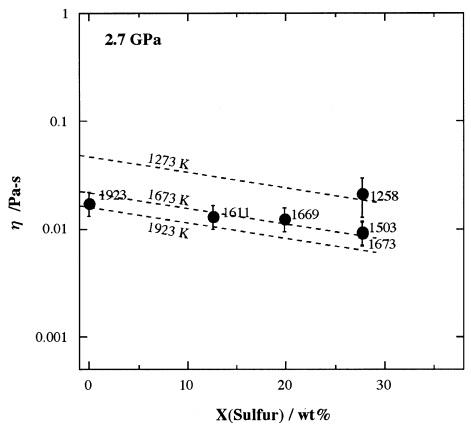

Fig. 6. Dependence of the viscosity coefficient on sulfur content. Solid circles show the original data at 2.7 GPa. Dashed lines represent the regression at 1273, 1673, and 1923 K and numbers show the run temperature.

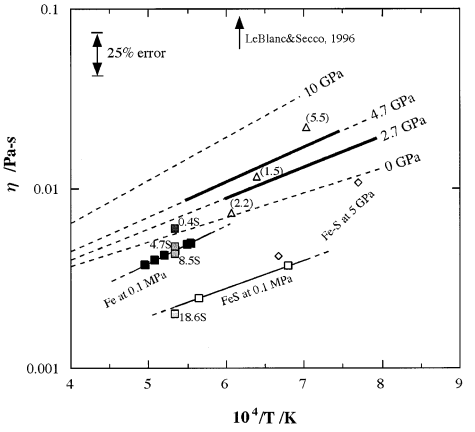

Fig. 7. Comparison of the viscosity data of this study with other data. Thick bold and dashed lines show the viscosity variation calculated by the present results. Upper ends of the dashed lines represent the eutectic temperatures of the corresponding pressures. Square symbols show the viscosity of Fe melt (solid squares; Lucas [5]), FeS melt (open squares; Barmin et al. [6]), and Fe–$Fe_{81}S_{19}$ melt (Vostryakov et al. [20]) at 0.1 MPa. Different pixel pattern in the square symbols represents the sulfur content (Numbers represent the sulfur contents). The data of Vocadlo et al. [21] at 5 GPa (open diamonds) are based on the Ab initio molecular dynamic calculation. The data of Dobson et al. [10] are also shown by open triangles with their experimentally investigated pressures in brackets.

4. Discussion

The present high pressure data are compared to the viscosity of liquid Fe [5], FeS [6], and intermediate composition of Fe–FeS (Vostryakov et al. [20]) measured at ambient pressure in Fig. 7. Ab initio molecular dynamics calculations were applied to the Fe–S melt at the conditions up to 5 GPa and 1500 K (Vocadlo et al. [21]). Their results are also shown in Fig. 7. Recently measured viscosities at high pressure by Dobson et al. [10] can be plotted in this viscosity range. All these data consistently suggest small pressure and compositional dependences of the viscosity. Only one exception is the results by LeBlanc and Secco [4], which reported the higher viscosities by 2–3 orders of magnitude at high pressures, outside the range of Fig. 7.

The empirical estimations from the liquid metal theory (Poirier [22]) provide additional support on the validity of the thermodynamic parameters of the present study. The linear empirical relationship between melting temperature (T_m) and activation energy (Q) or between atomic volume (V_{atm}) and activation volume (ΔV) for liquid metal has been found as:

$$Q \sim 22 T_m \sim 2.6 R T_m \quad (5)$$

$$\Delta V \sim 0.1\ V_{atm}. \quad (6)$$

Since T_m and V_{atm} are 1261 K and 9.6×10^{-6} m^3/mol respectively for the $Fe_{72}S_{28}$ alloy [3], these values become $Q = 27.3$ kJ/mol, and $\Delta V = 1.0\times10^{-6}$ m^3/mol. Those are quite consistent with the present result ($Q = 30.0 \pm 8.6$ kJ/mol, $\Delta V = (1.5 \pm 0.7)\times10^{-6}$ m^3/mol).

The effect of pressure, temperature, and sulfur content on the viscosity can be explained by the structural variation of the Fe–FeS melt. Viscosity decrease is generally caused by the structural relaxation, which is represented by the nearest neighbor distance (r_1) of the Fe–Fe bond in the compositional range between Fe and Fe–FeS eutectic. Structure analyses of the Fe–FeS eutectic and FeS melts were performed by Urakawa et al. [23,24] up to 7 GPa. According to their results, r_1 of the Fe–FeS melt increases with sulfur content, and r_1 naturally increases with the thermal expansion and the decompression, without any drastic structural change. The similar conclusion has been reached by Dobson et al. [25], on the basis of the measurements of the inter-diffusion coefficients of the Fe–FeS melt.

The viscosity values of LeBlanc and Secco [4] (0.5–14 Pa s at 1373–1573 K and 2–5 GPa) can not be accommodated with the present data (Fig. 7). As noted by themselves, the high viscosity value can only be explained by the data with drastic structural change of the Fe–FeS melt under high pressure. The results of the recent viscosity measurements ([9,10], and the present study), the diffraction studies [23,24], and the diffusion study [25] exclude such possibility, and the viscosity data reported by LeBlanc and Secco [4] are likely to be an experimental artifact.

By the comparison and combination of the present study with Dobson et al. [10], we can point out two issues on the activation energy and the compositional dependence of the Fe–FeS viscosity. Firstly, from their three data at different pressures (1.5, 2.2, and 5.5 GPa) they obtained a large activation energy ($Q = 100 \pm 5$ kJ/mol) by ignoring pressure effect. Pressure effect is not large but significant, as clarified in this study. We believe that our value ($Q = 30.0$ kJ/mol) should be preferred for the activation energy of the eutectic melt in the Fe–FeS system. Secondly, they concluded that the viscosity increases monotonously with sulfur content from the measurements on the FeS and $Fe_{73}S_{27}$ melts. Our study clarified the opposite tendency between pure Fe and $Fe_{72}S_{28}$. It is likely that the viscosity takes a minimum value at the eutectic point ($\sim Fe_{72}S_{28}$), because the near neighbor atomic pair changes from Fe–Fe pair to Fe–S pair at higher sulfur content [23]. Accordingly, sulfur content of the outer core is considered to be $S = 8$–11 wt%. [1], so that estimation of the outer core viscosity would require a revision.

5. Conclusion

The viscosity of Fe–FeS melt was measured by the X-ray radiography falling sphere method to

clarify the effects of pressure, temperature, and sulfur content. A new sample assembly enabled us to measure the viscosity at high temperatures with high accuracy. The results are summarized as follows:

1. Viscosity of the $Fe_{72}S_{28}$ melt was measured at conditions of 1233–1923 K and 1.5–6.9 GPa, respectively. The viscosity coefficients ranged from 8.0×10^{-3} Pa s up to 3.6×10^{-2} Pa s in these conditions.
2. The viscosity coefficient decreases slightly with increasing temperature, decreasing pressure, and increasing sulfur content. The activation energy (Q) and activation volume (ΔV) obtained from the present results are (30.0 ± 8.6) kJ/mol and $(1.5\pm0.7)\times10^{-6}$ m^3/mol, respectively, and the viscosity of the $Fe_{72}S_{28}$ melt is found to be smaller than that of the Fe melt by $15\pm10\%$. These tendencies can be well explained by the structural variation of the Fe–FeS melt.

Acknowledgements

The radiography experiments have been performed under contract of the SPring-8 (Proposal number: 1999B0023-ND-np and 2000A0287-ND-np). The authors are grateful to J. Reid, B. Poe, M. Kanzaki, K. Sato, M. Nakazawa, H. Kaneko, A. Yasuda, K. Mibe, M. Kurosawa, and N. Yagi for their collaboration of the radiography experiment and beneficial discussions. M. Akaishi helped us in preparation of the cell assembly at National Institute for Research in Inorganic Materials. The JEOL microprobe is a supported facility of the chemical analysis center, University of Tsukuba. We appreciate D. Dingwell, D. Dobson, and an anonymous reviewer for constructive comments.*[BW]*

References

[1] J.P. Poirier, Light elements in the Earth's outer core – a critical review, Phys. Earth Planet. Inter. 85 (1994) 319–337.
[2] A.E. Ringwood, Composition of the core and implications for the origin of the Earth, Geochem. J. 11 (1977) 111–135.
[3] T.M. Usselman, Experimental approach to the state of the core: part I. The liquidus relations of the Fe-rich portion of the Fe–Ni–S system from 30 to 100 kb, Am. J. Sci. 275 (1975) 278–290.
[4] G.E. LeBlanc, R.A. Secco, Viscosity of an Fe–S liquid up to 1300 °C and 5 GPa, Geophys. Res. Lett. 23 (1996) 213–216.
[5] L.-D. Lucas, Viscosite du fer pur et du systeme Fe–C Jusqu'a 4.8% C en poids, C. R. Acad. Sci. Paris 259 (1964) 3760–3767.
[6] L.N. Barmin, O.A. Esin, I.E. Dobroeinskij, Primenenie teorii reguljarnix rastvorov k opisaniju izoterm vjazkosti i moljarnix obemov binarnix suldnix rasplavov, Zh. Fiz. Khim. 44 (1970) 2560–2563.
[7] M. Kanzaki, K. Kurita, T. Fujii, T. Kato, O. Shimomura, S. Akimoto, A new technique to measure the viscosity and density of silicate melts at high pressure, in: M.H. Manghnani, Y. Shono (Eds.), High-pressure Research in Mineral Physics, Terrapub/AGU, 1987, pp. 195–200.
[8] D.B. Dingwell, Melt viscosity and diffusion under elevated pressures, Rev. Mineral. 37 (1998) 397–424.
[9] S. Urakawa, H. Terasaki, K. Funakoshi, T. Kato, A. Suzuki, Radiographic study on the viscosity of the Fe–FeS melts at the pressure of 5 to 7 GPa, Am. Mineral. 86 (2001) 578–582.
[10] D.P. Dobson, W.A. Crichton, L. Vocadlo, A.P. Jones, Y. Wang, T. Uchida, M. Rivers, S. Sutton, J.P. Brodholt, In situ measurement of viscosity of liquids in the Fe–FeS system at high pressures and temperatures, Am. Mineral. 85 (2000) 1838–1842.
[11] W. Utsumi, K. Funakoshi, S. Urakawa, M. Yamakata, K. Tsuji, H. Konishi, O. Shimomura, SPring-8 beamlines for high pressure science with multi-anvil apparatus, Rev. High Pressure Sci. Technol. 7 (1998) 1484–1486.
[12] S. Urakawa, M. Morishima, T. Kato, A. Suzuki, O. Shimomura, Equation of state for h-BN, Photon Fact. Act. Rep. G275 (1993) 383.
[13] H. Faxen, Gegenseitige einwirkung zweier kugelen, die in einer zähen flüssigkeit fallen, Ark. Mat. Astron. Fys. 19 (1925) 1–8.
[14] W.D. Kingery, Property measurements at high temperatures, John Wiley and Sons, New York, 1959, 416 pp.
[15] J.C. Jamieson, J.N. Fritz, M.H. Manghnani, Pressure measurement at high temperature in X-ray diffraction studies: Gold as a primary standard, in: S. Akimoto, M.H. Manghnani (Eds.), High-pressure Research in Geophysics, Center for academic publishing, Tokyo, 1982, pp. 27–48.
[16] R.G. McQueen, S.P. Marsh, J.W. Taylor, J.N. Fritz, W.J. Carter, The equation of state of solids from shock wave studies, in: R. Kingslow (Ed.), High-velocity Impact Phenomena, Academic press, New York, 1970, pp. 249–419.
[17] M. Nagamori, Density of molten Ag–S, Cu–S, Fe–S, and

Ni–S systems, Trans. Metall. Soc. AIME 245 (1969) 1897–1902.
[18] R.S. Hixon, M.A. Winkler, M.L. Hodgdon, Sound speed and thermophysical properties of liquid iron and nickel, Phys. Rev. B 42 (1990) 6485–6491.
[19] C. Sanloup, F. Guyot, P. Gillet, G. Fiquet, M. Mezouar, I. Martinez, Density measurements of liquid Fe–S alloys at high-pressure, Geophys. Res. Lett. 27 (2000) 811–814.
[20] A.A. Vostryakov, N.A. Vatolin, O.A. Yasin, Viscosity and electrical resistivity of molten alloys of iron with phosphorous and sulphur, Fiz. Metal. Metalloved. 18 (1964) 476–477.
[21] L. Vocadlo, D. Alfe, G.D. Price, M. Gillan, First principles calculations on the diffusivity and viscosity of liquid Fe–S at experimentally accessible conditions, Phys. Earth Planet. Inter. 120 (2000) 145–152.
[22] J.P. Poirier, Transport properties of liquid metals and viscosity of the Earth's core, Geophys. J. 92 (1988) 99–105.
[23] S. Urakawa, N. Igawa, K. Kusaba, H. Ohno, O. Shimomura, Structure of molten iron sulfide under pressure, Rev. High Pressure Sci. Technol. 7 (1998) 286–288.
[24] S. Urakawa, K. Funakoshi, O. Shimomura, H. Ohno, T. Kikegawa, Structure of molten iron–sulfur alloys at 3 GPa, submitted.
[25] D.P. Dobson, J.P. Brodholt, L. Vocadlo, W.A. Crichton, Experimental verification of the Stokes–Einstein relation in liquid Fe–FeS at 5 GPa, Mol. Phys. 99 (2001) 773–777.